THE SELECTION OF ELECTRICAL ANALOG COMPONENTS FROM COMPUTATIONAL MODEL IMPEDANCE SPECTRA

Lucy Perkins Phelps

A thesis submitted to the faculty of the University of North Carolina at Chapel Hill and North Carolina State University in partial fulfillment of the requirements for the degree of Master of Science in the Joint Department of Biomedical Engineering.

Chapel Hill
2010

Approved By:

Dr. Brooke Steele

Dr. Shawn Gomez

Dr. Carol Lucas

ABSTRACT

LUCY PERKINS PHELPS: The Selection of Electrical Analog Components from Computational Model Impedance Spectra
(Under the direction of Dr. Brooke Steele)

Lumped parameter models can be used as accurate boundary conditions in hemodynamic modeling, requiring only the estimation of a few physiologically relevant parameters. The best way to estimate these parameters (typically resistances and capacitances) has seen much investigation, but all current techniques require experimental (or periodic time-domain) blood pressure or blood flow data. A method that can estimate lumped parameter model components using only impedance spectra would widen the scope of usefulness for lumped parameter models as boundary conditions. Their usefulness would then include cases where such data cannot be obtained. The methods presented in this work estimate the resistance and capacitance values of two- and three-element Windkessel models using only features found in typical impedance spectra. Comparing these methods to “gold standard” pressure and flow data, each other, and previously published methods can determine the accuracy of a ‘Fourier-domain only’ strategy.

DEDICATION

I would like to dedicate this work to a few of the people who have most supported me, through both my trials and successes, and that have helped me to reach this point in my academic career:

My husband, Luke, who is my everything,

My sister, Elle, who is my happiness,

Amy, who is my sanity,

and in memory of my mom.

ACKNOWLEDGEMENTS

I would like to thank Dr. Brooke Steele, my advisor, for her patience and guidance throughout my time as a graduate student.

I would like to thank my committee, Dr. Carol Lucas and Dr. Shawn Gomez, for their support.

I would also like to thank Rachel, for being a student mentor who was always willing to help or talk things through.

Lastly, thanks to my family (immediate, extended, and in-laws), all my success I owe to you.

Table of Contents

LIST OF TABLES

Table

LIST OF FIGURES

Figures

ABBREVIATIONS AND SYMBOLS

IMA	Inferior Mesenteric Artery
P	Pressure
Q	Flow
SMA	Superior Mesenteric Artery
Z_{ch}	Characteristic Impedance

CHAPTER I

INTRODUCTION AND BACKGROUND

1.1 Motivation

Hemodynamic modeling is becoming an increasingly beneficial tool for cardiovascular surgical planning and diagnostics. As cardiovascular diseases play a role in more than half the deaths in the United States [1], it is important for these tools to be as robust and accurate as possible. Being able to quantify parameters such as resistance and compliance of blood vessels through vascular networks allows for hemodynamic models that represent blood flow and blood pressure through a particular systemic vasculature. The accurate implementation of boundary condition models is imperative for hemodynamic modeling, where precise representation of physiologic conditions is required for yielding a useful tool. Two- and Three- element lumped parameter, or Windkessel, models have consistently been useful for modeling hemodynamic boundary conditions [2-5]. These models require initial estimation of two or three parameters. The motivation for this project was to develop a new method for estimating these parameters to increase the usability of these types of models.

1.2 Cardiovascular System

The cardiovascular system is composed of the heart and the circulatory system. The heart acts as a pump, generating pressure that circulates blood throughout the circulatory system to the tissues and organs of the body. The circulatory system is divided into two circuits, the pulmonary circulation and the systemic circulation. The pulmonary circulation delivers blood from the heart to the lungs and back to the heart. The systemic circulation consists of the blood vessels that carry oxygenated blood throughout the rest of the body.

1.2.1 Systemic Circulation

Arteries are the blood vessels of the systemic circulation that carry blood away from the heart, delivering oxygen and nutrients. Arteries are composed of a thick smooth muscle layer and large amounts of elastic and fibrous connective tissue. Arteries form a branching pattern throughout the body, dividing into smaller and smaller arteries. Eventually these arteries become arterioles and capillaries, the smallest vessels in the cardiovascular system. The capillaries join with venules and are the site of gas and nutrient exchange for the systemic circulation. Then, oxygen poor blood returns to the heart via the body's venous system [1].

In the scope of this project, nine of the major arterial branches are discussed. These are the renal, celiac, iliac, superior mesenteric (SMA), inferior mesenteric (IMA), internal iliac, external iliac, profunda and common femoral arteries. The locations of these can be seen in Figure 1 as part of the overall systemic circulation.

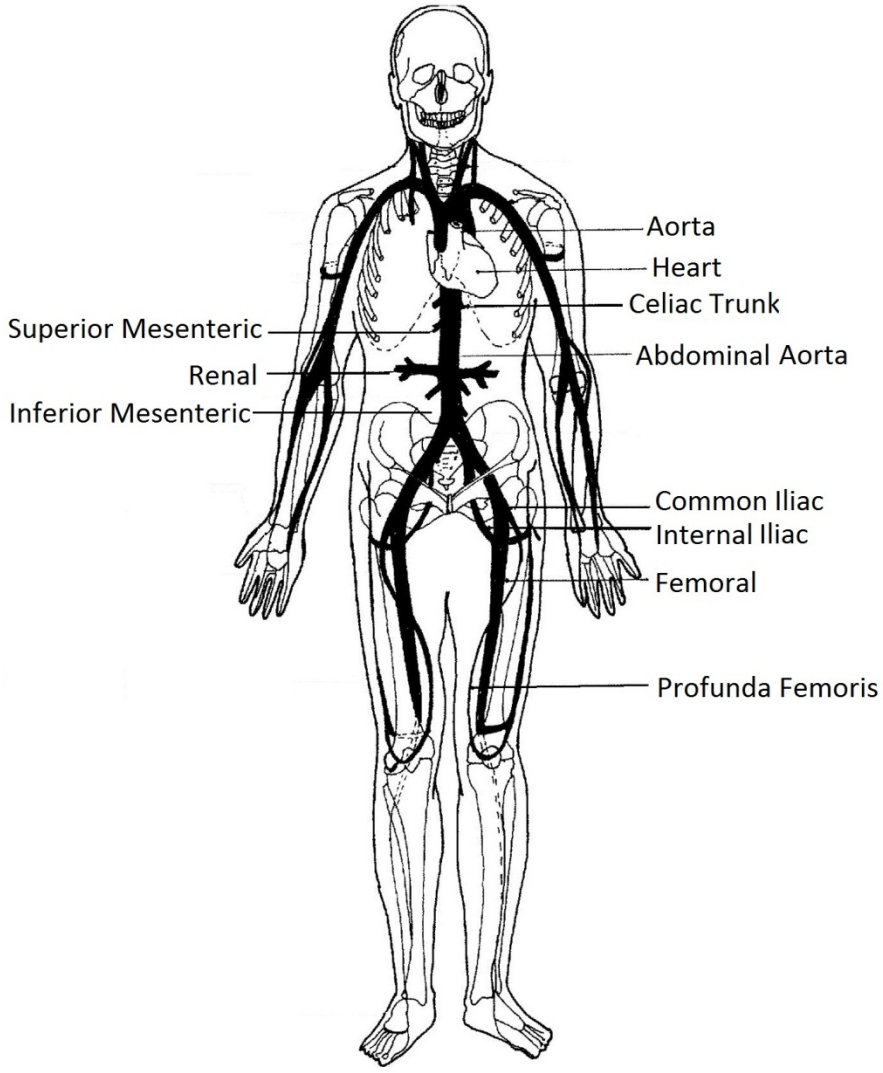

Figure 1: Major Arteries of the Viscera and Lower Extremities *- modified from figure found at http://www.answers.com/topic/artery*

1.2.2 Blood Flow

Typical blood flow through the systemic circulation reflects the ventricular contraction of the heart as the cardiac cycle goes from systole to diastole and repeats. Figure 2 shows these typical waveforms. Cardiac output (heart rate times stroke volume) can be calculated as an indicator of total blood flow through

the body. However, it yields no insight as to how that blood is distributed throughout the arterial system. Hemodynamic models are useful in characterizing blood flow where experimental data cannot be extracted. Knowing the resistive and compliance characteristics of a particular arterial network allows insight about the blood flow and pressure through the vasculature in question. As previously mentioned, the arterial system forms a branching pattern throughout the body. As the size (radius) of the arteries decrease, the walls of these blood vessels become much less elastic [1]. This loss of elasticity, or compliance, combined with blood viscosity and the length of the blood vessels create the resistance to blood flowing through the branching arteries.

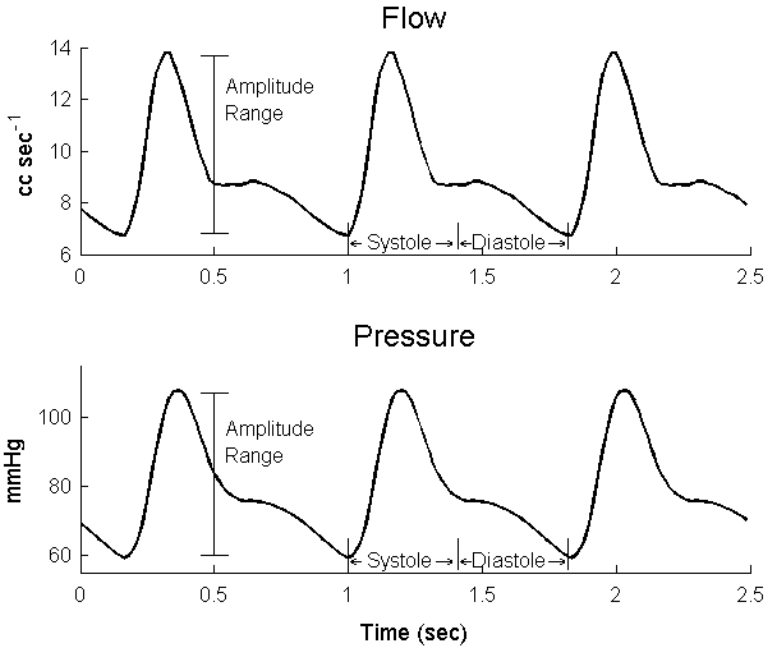

Figure 2: Typical Blood Flow and Pressure Waveforms- *This figure shows the amplitude range of blood pressure and blood flow cycles (at rest). The systolic increase of pressure and flow vs. the diastolic 'rest' is also depicted. These are parameters that can be used to compare like waveforms.*

1.2.3 Blood Pressure

Blood is propelled throughout the systemic circulation by the heart. The ventricles of the heart contract creating the pressure which drives blood through the arteries (Figure 2). Blood flows from high to low pressure and the flow is inversely proportional to the resistance of the blood vessels [1]. During exercise negative flow that exists during rest conditions is eliminated due to increased heart rate and cardiac output [6]. During exercise, cardiac output increases (going from approximately 5 L/min to 30-35 L/min for a healthy person with resting heart rate of 72 bpm) [1]. During rest or exercise, the geometry of arterial networks, changes in vascular anatomy (dilation or constriction of the vessels) and the resistive and compliance characteristics of vessels are all parameters that are considered in hemodynamic models that yield accurate representations of blood pressure and flow.

1.3 Computational Models of Systemic Circulation

Accurate mathematical models represent the true physiological behaviors of vascular networks. There are many types of hemodynamic models, with one-dimensional and three-dimensional finite element analysis models being two of the most useful. These models characterize blood flow and blood pressure though a particular region of interest in a vascular network. Everything outside of this region of interest is then represented with boundary conditions [6].

Two types of boundary condition models that are extensively used for this application are geometric and lumped parameter impedance boundary conditions. Geometric, or anatomically based distributed models, represent a vascular network by assuming a specific geometry (such as a structured branching tree) and computing impedance [6, 7]. Lumped parameter models represent an arterial system as an electrical circuit inputting blood flow as current or blood pressure as voltage. Both types of models allow characterization of blood flow and pressure data for the circulatory system outside of the arterial network being studied, and are good boundary conditions for this application.

1.3.1 Boundary conditions

Boundary conditions can quantify blood flow and pressure characteristics at the input or output of a particular vascular network. In hemodynamic modeling they represent the behavior of vasculature outside of the region being examined. This allows a region of interest to be modeled and the rest of the circulatory system to be represented with only a few parameters. As previously mentioned, a good boundary condition parameter is vascular input impedance [7]. Impedance allows behavior regarding blood pressure, blood flow, and arterial wall properties to be extracted. Impedance of a vascular network can be determined using both geometric and lumped-parameter models. Using impedance as a common boundary condition, we can use ‘gold standard data’, computed using a geometric model, to compare different lumped parameter models.

1.4 Impedance

Vascular input impedance is a parameter that can be used to characterize an arterial system, representing the opposition to periodic blood flow. Defined as the ratio of blood pressure to blood flow, the input impedance is a complex quantity which illustrates flow as a response to a pulsatile pressure [8]. Impedance is determined by the geometric and vascular structure of the arterial network in question. It can represent a basic lumped parameter model or a more complex branching geometry [9]. Impedance is defined in the frequency domain. A similar general shape of the impedance modulus and phase spectra can be observed in any branching structure despite the number of branches or terminals. A typical impedance modulus starts at a high peripheral resistance and then rapidly decreases before oscillating at higher frequencies. A typical phase spectra will rapidly decrease from zero, reach a minimum point, and then recover to oscillate around zero at higher frequencies [9]. This general pattern can be observed in Figure 3 and is also discussed in the work of Mills et all [10] where the impedance shapes were computed from experimental data for several of the major systemic arteries.

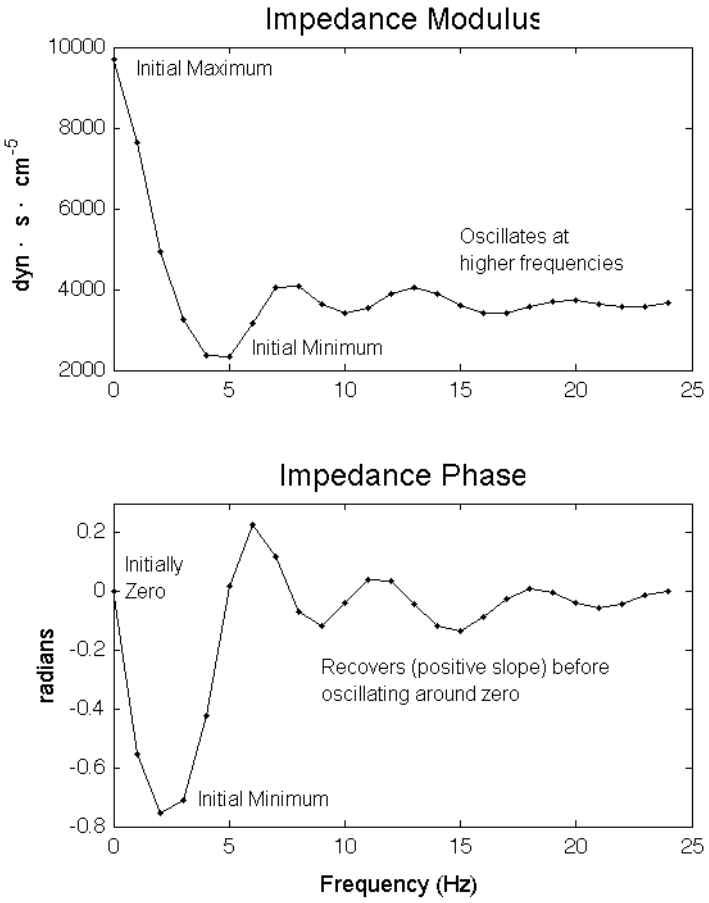

Figure 3: Typical Shape of Impedance Modulus and Phase

The oscillations at the higher frequencies indicate the effects of the different geometries of vascular systems, as different geometries would create different wave reflections [8, 9]. The definition of impedance describes a linear relationship; given an impedance spectra with an input of blood flow, blood pressure could be extracted with identical frequency, though there is a phase shift (and vice versa, with an input of pressure, flow could be determined). This

makes impedance a good validating parameter for both lumped parameter and geometric models [9].

1.5 Lumped Parameter Models (Electrical Analogs)

In the two-element Windkessel model, originally proposed by Otto Frank in 1889 [11], the resistor represents the resistance (as dictated by vessel size, so a network consisting of smaller vessels would have a greater resistance to flow than a network of larger vessels) and the capacitor represents the total arterial compliance of the systemic vascular bed in question. An example of this is shown in Figure 4(a). As a lumped parameter model represents an arterial network through a pressure-flow relationship at the entrance to the vasculature in question, the wave travel aspects (such as damping, amplification, etc) inside the modeled network cannot be examined. These wave reflections are illustrated in experimental impedance spectra as the higher frequency oscillations (Figure 4). These oscillations are not present in two-element lumped parameter model impedance spectra, where the modulus decays to negligible values [2, 12]. It was also shown by Stergiopulus that the two-element Windkessel model can be used to illustrate blood flow and pressure behavior not only for the entire arterial tree, but also as a representative of smaller, downstream arterial networks with constant compliance [12].

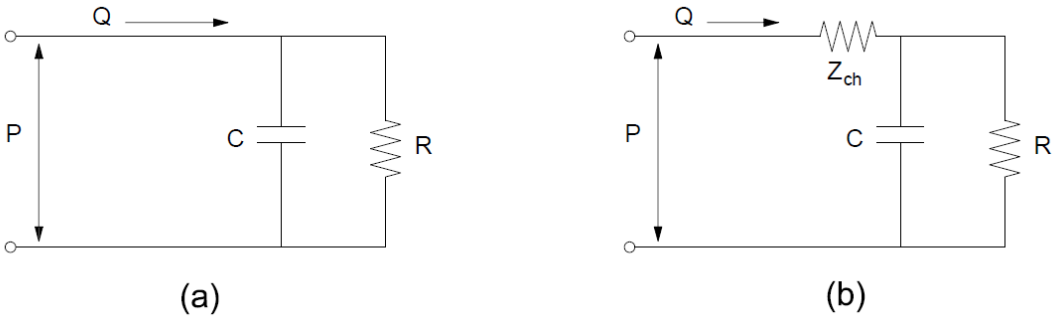

Figure 4: Two- and Three- Element Windkessel Models (Electrical Analog) *- a) Two-element Windkessel model where R represents the total resistance and C represents the compliance of an arterial network. b) In a three-element Windkessel Model the Z_{ch} is added to the circuit as a resistor.*

The three-element Windkessel model adds the parameter of characteristic impedance, which is typically represented by a second resistor in the electrical analog. This is shown in Figure 4(b). The characteristic impedance (Z_{ch}) added to the peripheral resistance (R) comprises the total equivalent resistance. This characteristic impedance parameter allows the model to better represent the higher frequency characteristics, though the oscillations are still not present. This parameter is described as the wave speed multiplied by blood density divided by cross-sectional area (or $Z_{ch} = \frac{\gamma\rho}{A}$ where A is aortic cross-sectional area when referring to aortic impedance, etc.) and its addition is often seen as an improvement over the two-element lumped parameter model [2]. This model is practical and easily understood, as all parameters represent actual physiological counterparts (e.g. capacitance represents compliance) [4]. Although there are documented shortcomings, such as the tendency to underestimate the

characteristic impedance and overestimate the total arterial compliance [13, 14], the three element Windkessel is generally accepted to be a useful compromise between accuracy and complexity. In *The Arterial Windkessel*, Westerhof et al. [2] concludes that the three-element Windkessel model can adequately describe the pressure-flow relations at the entrance of a systemic arterial system.

Because low frequency errors can occur with the three-element Windkessel model, which can be attributed to the inclusion of the characteristic impedance, four-element models have been examined. Typically this includes an inertance in series with the characteristic impedance but this inertance was seen to be extremely difficult to estimate [2]. For the applications investigated in this project the two- and three-element models were deemed more appropriate.

1.5.1 Impedance of Windkessel Model

A lumped parameter or Windkessel model, representing a downstream arterial system, can be used as a boundary condition when modeling a larger vascular network. Typically a three-element model, the frequency-dependent impedance of such a boundary condition can be computed as seen in Equation 1 [14].

$$Z(0,\omega) = \frac{R_1 + R_2 + i\omega C R_1 R_2}{1 + i\omega C R_2} \tag{1}$$

The impedance of lumped parameter models do not have the same shape as the aforementioned typical experimental impedance models as they lack the oscillations at higher frequencies (wave reflections).

1.6 Parameter Estimation

Parameter estimation for lumped parameter models has been extensively investigated. The peripheral resistance is typically represented as the initial ratio of pressure to flow [2, 15]. However there have been many ways of estimating the total arterial compliance and the characteristic impedance.

In *The Arterial Windkessel*, Westerhof et al [2] outlines eight different estimation methods for the total arterial compliance. Some of the more current and most commonly used examples are summarized as follows. The ‘Pulse Pressure method’ fits systolic and diastolic pressure computed with a two-element Windkessel and measured flow data, to measured pressure data. The ‘Parameter Estimation Method’ uses three-element Windkessel and measured flow data to predict pressure data. This is then compared to measured pressure data, minimizing the difference between the two. The inverse is also used to predict flow data given measured pressure data. The ‘Input Impedance Method’ carries out similar comparisons but is performed in the frequency domain, comparing impedance spectra of computed vs. measured data. The ‘Area Method’ estimates RC as being the area under the diastolic pressure divided by the pressure difference between start and some endpoint. This gives an estimate for two-element lumped model parameters and then to the characteristic impedance would be estimated separately to apply this method to a three-

element model. Several other parameter estimation strategies are also described and the limitations and advantages of each are briefly discussed. All the strategies for estimating arterial compliance rely on measured pressure or flow data [2].

No current methods for estimating this parameter solely use Fourier domain data. Several sources do point out that compliance is a low-frequency property, so the best compliance estimation methods should utilize the lowest frequencies [13, 16].

The most accurate way of estimating the characteristic impedance has also been examined. Typically this parameter, characterized by a second resistor, is estimated by averaging input impedance modulus values over a particular range of frequencies [17, 18], though the definition of that range is somewhat ambiguous. It has also been approximated using slopes of pressure and flow waveforms during early systole [17].

One current limitation of using the lumped parameter boundary conditions is that the most accurate current parameter estimation strategies require experimental data. A particular focus of this work is to investigate parameter estimation strategies that require no time domain data, selecting all RC and RCR parameters from impedance spectra.

In 1994, Shim et al presented a three-element Windkessel parameter estimation method that could be implemented solely using time-domain calculations [4]. This method is based on integrating the governing differential

equations of the three-element Windkessel. These are shown in Equations 2, 3 and 4.

$$Z_{ch} = \frac{1}{m}\sum \frac{PPA(t_k)}{Q(t_k)} \tag{2}$$

$$R = \frac{P_{mean}}{Q_{mean}} - Z_{ch} \tag{3}$$

$$C = \frac{\int_{t_1}^{t_2} P_{avg}(t)dt - (R + Z_{ch})\int_{t_1}^{t_2} Q_{avg}(t)dt}{R(P_{avg}(t_1) - P_{avg}(t_2)) - RZ_{ch}(Q_{avg}(t_1) - Q_{avg}(t_2))} \tag{4}$$

The accuracy of this method was examined by comparing it with four previously published methods. The pressure and flow waveforms were reconstructed using all methods of estimating the Windkessel parameters and were compared back to experimental flow and pressure waveforms [4]. It was concluded that this method performed as well as the other known strategies.

1.7 Specific Aims

Similar to the comparisons made by Shim et al, we can conduct pressure and flow waveform comparisons of several methods of Windkessel parameters estimation that depend solely on Fourier domain data. Implementation of an

accurate method that can estimate lumped parameter model components using only impedance spectra would eliminate the need for periodic time domain or experimental data altogether. This would widen the scope of usefulness for lumped parameter models to include cases where such data is unavailable. The methods presented in this work estimate the resistance and capacitance values of two and three-element Windkessel models using only features found in typical impedance spectra. Comparing these methods to “gold standard” pressure and flow data, as well as to each other and previously published methods can determine the accuracy of a ‘Fourier-domain only’ strategy.

CHAPTER II

METHODS

Initially three-element lumped parameter models were investigated. First this study compared three different methods of selecting a characteristic impedance value (Z_{ch}, or R_1 for simplicity) and deriving a peripheral resistance (R_2) and compliance value (C). The goal was to establish an accurate parameter selection method based on features present in an impedance modulus and phase. The computational model of the blood vessels of the viscera and lower extremities developed in Steele, et al [6] is used in this work. Eighteen impedance spectra of the peripheral vessel outlets were examined during both rest and exercise conditions to provide a wide range of impedance moduli and phase characteristics for comparison. The lumped parameter model components were selected for each spectrum using the methods described below, and pressure and flow data were reconstructed using the selected RCR components. The reconstructed waveforms were then compared to the "gold standard" computational model data to determine the most simple and accurate method of selecting RCR components from impedance spectra data. A similar strategy added two-element Windkessel models to the comparison. Results from

comparisons of both models are compared to previously established parameter estimation methods.

2.1 Gold Standard Impedance Spectra

In order to compare the different methods for selecting the RCR components, previously developed one-dimensional (1D) finite element analysis (FEA) software [19] was used to model the visceral and peripheral blood flow and pressure. The outlet boundary conditions were specified with structured tree parameters for each outlet for both rest and exercise conditions [6]. The impedance spectrum for each was then computed using Womersley's method of calculating impedance for oscillatory flow in an elastic tube [20] and the structured tree parameters as described in detail by Olufsen, et al [6, 14].

The resulting impedance calculations provide a "gold standard" by which to compare the methods of selecting the RCR or RC values. The method which selected RCR or RC values that could then be used to reproduce the most accurate flow or pressure waveforms (compared to the original flow and pressure data from Steele, et al [6]) would constitute the best method of selecting lumped parameter model components directly from impedance data.

2.2 Three Element Lumped Parameter Model

2.2.1 Estimation of Characteristic Impedance (R_1)

A typical impedance modulus will have an initial maximum value (typically the zero frequency value or equivalent resistance), then will decrease to a minimum. After the minimum has been reached, the values will oscillate at higher frequencies for experimental and structured tree moduli spectra (such as in Figure 3) or exponentially approach the characteristic resistance for lumped parameter modulus spectra (such as in Figure 6).

Traditionally, estimating the value of R_1 has been defined as averaging the higher frequency terms of the impedance modulus as previously described. As this strategy can sometimes be ambiguous, a more defined method would lead to a more consistent estimation procedure. Three methods of specifying the R1 value using only features present in typical impedance are investigated in this study. Method 1: the proximal resistor (R_1) is set to a minimum modulus value (Figure 5a). This yields a lower characteristic impedance value than is typically seen. Method 2: the proximal resistor (R_1) is set to the average of the higher order modulus terms after the minimum modulus value (Figure 5b). This is a more classical method of characteristic impedance selection. Method 3: the proximal resistor (R_1) is set to the average of the modulus terms up to the term in which the phase angle of the impedance spectra changes slope (Figure 5c). This method yields a higher value for the characteristic impedance than is typically seen.

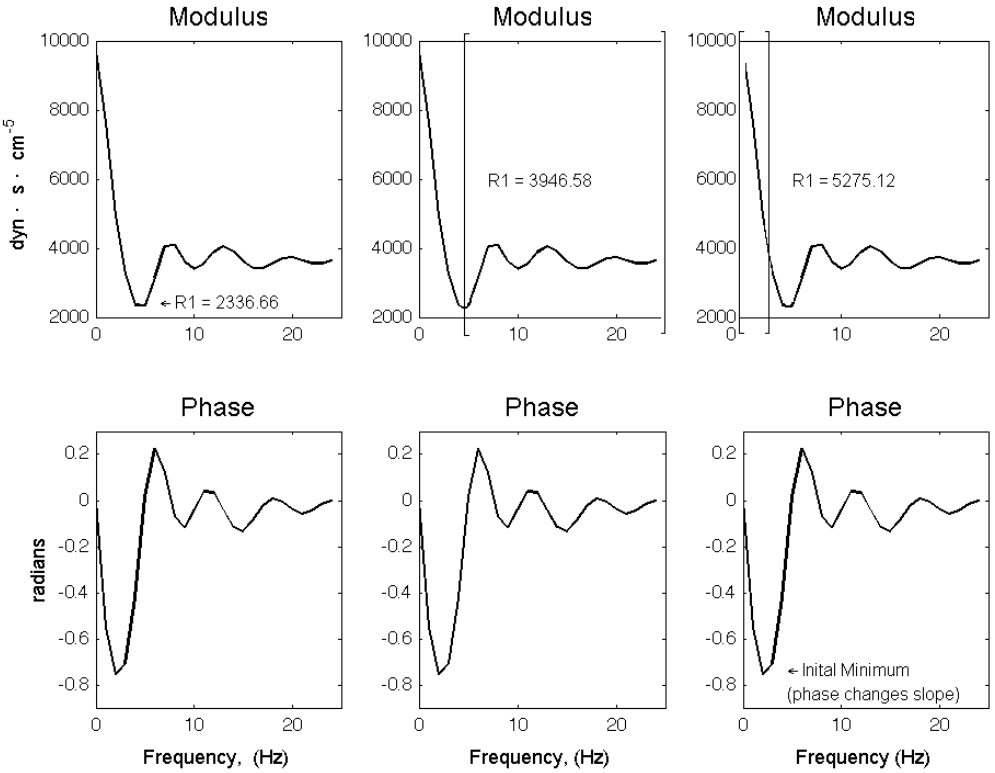

Figure 5: Three Methods for Selecting the R_1 Parameter: *5a) Method 1: the proximal resistor (R_1) is set to a minimum modulus value 5b) Method 2: the proximal resistor (R_1) is set to the average of the higher order modulus terms after the minimum modulus value 5c) Method 3: the proximal resistor (R_1) is set to the average of the modulus terms up to the term in which the phase angle of the impedance spectra changes slope*

2.2.2 Estimation of Peripheral Resistance (R2)

The equivalent resistance is the sum of the two resistances in a three-element Windkessel model ($R_e = R_1 + R_2$). The zero frequency value can be taken directly from the impedance data, therefore once the R_1 resistor was estimated the R_2 resistor was calculated.

2.2.3 Intermediate Methods -Dynamic Optimization of Capacitance

Once the resistance values were chosen, the capacitance values are selected by minimizing the amplitude error, reproducing accurate diastolic means, and replicating the wave shape between the reconstructed flow and pressure waveforms and the original data. Custom software allowed the dynamic altering of a capacitance value for error minimization, using the resistance values from each method described above.

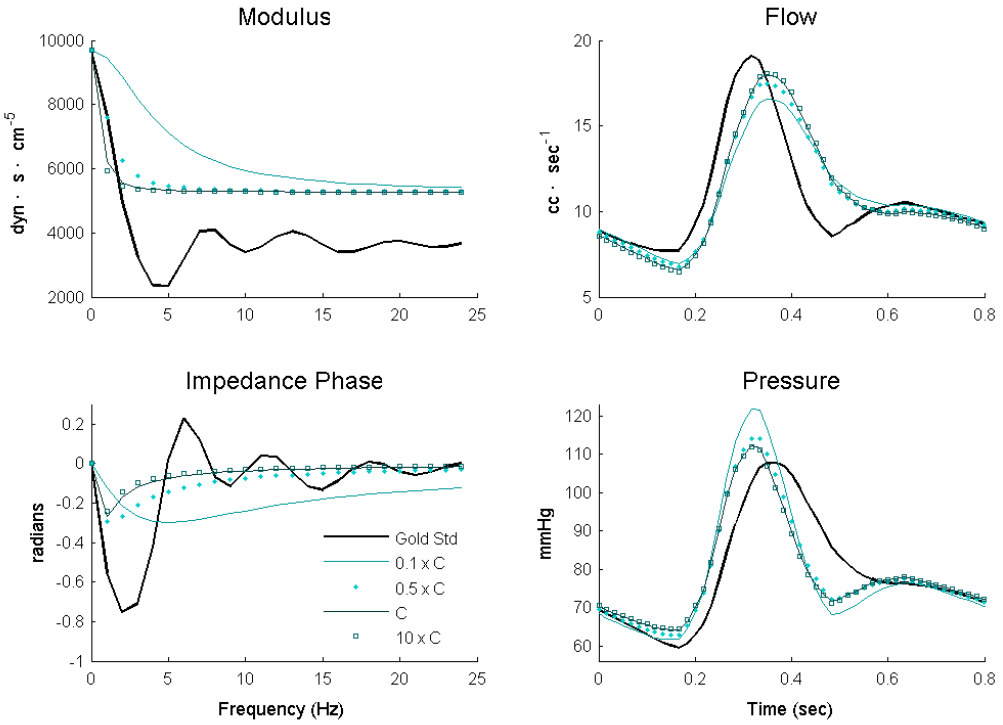

Figure 6: Effects of Changing C on Flow and Pressure Waveforms *– Dynamic selection of C allows for the important characteristics of the modulus and phase spectra to be identified. Recovery time of the phase curve increases accuracy of flow and pressure reconstructions (Example uses computed Celiac Flow data under rest conditions as the Gold Standard, where C (best fit) is estimated at 8.085 x10^-5 cm^5/dyne*s)*

The capacitance value that minimizes the error between the original and the reconstructed pressure or flow waveforms as selected. The method with the lowest error was determined to be the best method for selecting the resistance components (or, optimizing error values by dynamically choosing C allows comparison of the selection methods of R_1 and R_2). This "best" method of selecting the resistance values can then be used in determining the features of the impedance spectra that are important for computing a capacitance value.

2.3 Intermediate Results

2.3.1 Determining Resistance Selection Method

Reconstructed flow and pressure waveforms for all eighteen outlets, using each selection method, are compared to original "gold standard" data. Comparisons of the precision and the shape of the reproduced curves indicate the best parameter estimation method. Amplitude Range Error (Amplitude Error), which is calculated as the difference between the computed and experimental amplitude ranges, as well as difference in the diastolic mean, and frequency of waveforms, are parameters used to compare the test reconstructions to the original computational data. From these quantifiers, the "most accurate" method will be the most precise replica of the original data that does not negate the effects of conditions such as hypertension, hypotension, etc., that may be present in a subject's original blood flow or pressure data.

2.3.2 Comparison of Flow Waveforms

Resistance components were initially selected using three trial methods, and a capacitance value that was dynamically selected to minimize error between reconstructed flow waveforms and the original “gold standard” flow data. Method 3 yielded the most accurate results when optimizing a capacitance value. Method 2 and Method 3 were generally comparable except Method 3 showed a smaller time lag between the Gold Standard data and the reconstructed waveforms. For Method 3, the diastolic mean was reconstructed to within 5% (average of all outlet cases) under rest conditions and within approximately 3.5% (average of all outlet cases) under exercise conditions. Amplitude range error was the lowest for Method 3 in sixteen of the eighteen test cases. The average amplitude rage error for all cases was less than 3%. Figure 7 illustrates examples of these flow comparisons.

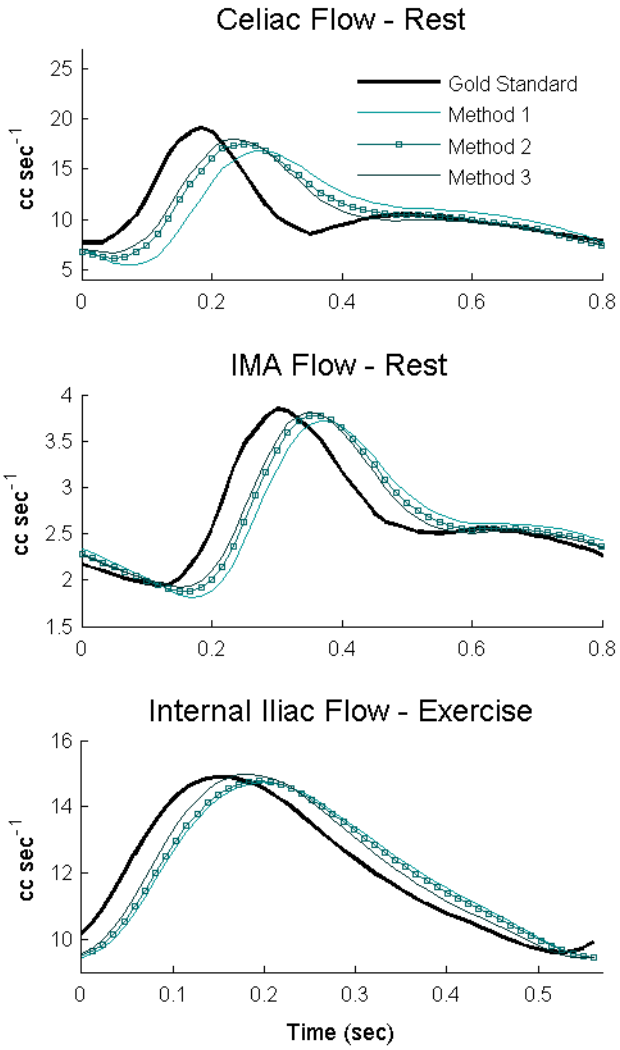

Figure 7: Examples of Flow Comparisons – *The flow waveforms reconstructed using all methods are compared to the computed gold standard data. IMA and Celiac arterial flow under rest conditions and Internal Iliac flow under exercise conditions are shown as examples.*

2.3.3 Comparison of Pressure Waveforms

The same comparison techniques were used to examine reconstructed pressure waveforms. Components were selected in the same manner and the

same error comparisons were considered. The diastolic mean pressures were reconstructed to within 2.5% (average of all outlet cases) under rest conditions and within 2% (average of all outlet cases) under exercise conditions. There was not a significant difference in the values between the three methods; all were determined to perform adequately in reconstructing the diastolic mean pressure. In terms of Amplitude Error, Method 3 was again the most accurate method in 16 of the 18 tested cases. Over all cases, using selection Method 3, the amplitude error was still less than 1%. The superior mesenteric artery and the internal iliac artery outlets under rest conditions were the same two outliers in comparisons of both pressure and flow reconstructions. Figure 8 shows examples of pressure waveform comparisons.

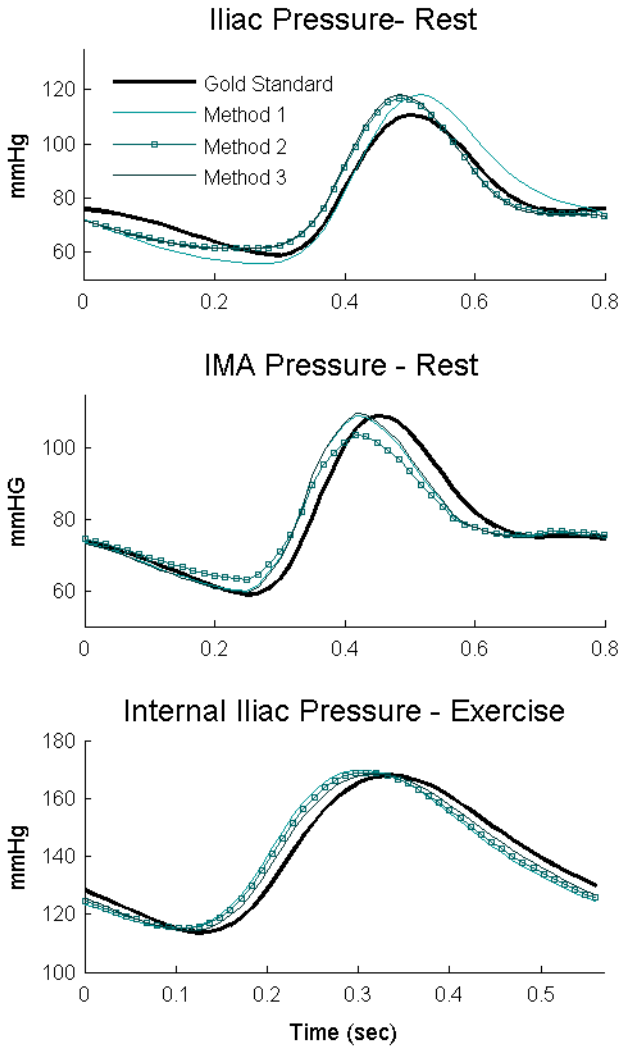

Figure 8: ***Examples of Pressure Comparisons –*** *The pressure waveforms reconstructed using all methods are compared to the computed gold standard data. Iliac and IMA arterial pressure under rest conditions and Internal Iliac pressure under exercise conditions are shown as examples.*

2.4 Final Studies - Impedance Spectra Estimations of Capacitance

While an RCR phase spectra may differ significantly from an experimental/ structured tree phase spectra, both will start around zero and have an initially

negative slope before reversing to a positive slope. For an RCR phase spectrum, the phase angle will then exponentially approach zero, while an experimental phase angle may oscillate and become positive. By examining the impedance spectra that produced the most accurate flow and pressure reconstructions, several notable observations about the phase were made. These observations were used to identify important graphical characteristics of the "best" RCR impedance phases so as to help develop a method to best estimate a *C* value.

The reconstructed vs. original flow waveforms, illustrated that the recovery time of the impedance phase after the initial minimum is important and should play a role in capacitance value selection. Upon examination of several impedance spectra, it appeared that the intersection of an impedance phase produced by the "best" method of resistance selection and the original "gold standard" impedance curves would be approximately close to a value that minimized this settling time. So to estimate *C*, equation 5 was implemented in software.

$$C = \left| \frac{Z - R_1 - R_2}{\omega R_1 R_2 i - Z i \omega R_2} \right| \tag{5}$$

Here ω is the chosen frequency (intersection of phase curves – determined to be approximately 2/3 the peak to peak of the initial positive sloping phase), R_1 and R_2 are previously estimated and Z and Zi are the impedance modulus and phase values at the chosen frequency.

2.5 Two-Element Lumped Parameter Model

Though a three-element lumped parameter model is typically depicted as being superior to the two-element model for this application, the two-element Windkessel is simpler to implement. Therefore if it can achieve similar or even better results, then its usefulness may be re-evaluated. As this is a novel approach to parameter estimation, both two- and three-element Windkessel models are examined.

2.5.1 Estimation of (total) Peripheral Resistance (R)

As previously described, the two-element Windkessel Model excludes the characteristic impedance found in the three-element model. Here the resistance value is the initial ratio of the blood pressure to blood flow, or the first harmonic value of the impedance modulus (the initial maximum of a typical modulus). This is easily included in the software as zeroing the R_1 term.

2.5.2 Estimation of Capacitance (C)

Similar to the three-element lumped parameter estimation strategies, the capacitance value can be estimated by solving the corresponding circuit

equations. In the two-element case this simplifies to Equation 6 where components are estimated as presented in the three-element case above:

$$C = \left| \frac{R - Z}{Zi\omega R} \right| \tag{6}$$

These impedance moduli and phase, for the two-element model, will have a different typical shape than either three-element, or experimental impedance spectra. The impedance modulus will exponentially approach zero from the initial maximum, and the phase plot will not recover after reaching its initial minimum. Again, pressure and flow can be reconstructed from the estimated components and compared to the three-element model reconstructions and the "gold standard" data.

2.6 Comparison of Fourier Domain Method to Time Domain Method

For completeness, selecting RCR and RC components using the aforementioned methods can be compared not only to the "gold standard" data, but also to the 'time domain method' described and validated by Shim et al [4]. The Shim et al equations (2, 3, and 4) were implemented in software to provide this additional comparison. Parameters were estimated for all outlets using this 'time domain method' and comparisons were again performed between the reconstructed flow and pressure waveforms and the original "gold standard" flow and pressure waveforms at each outlet.

CHAPTER III

RESULTS

3.1 Three-Element Lumped Parameter Model

3.1.1 Selection of Resistance Values – Intermediate Step

The best method of selecting the resistance components is validated in the intermediate step of the methods section. This determined that Method 3 is the most accurate at reproducing flow and pressure waveforms from a given impedance spectra using an optimized capacitance. Examples of the values chosen for resistance and capacitances for all methods are shown in Table 1.

3.1.2 Selection of Capacitance Values - Final Studies

Once resistance values are determined, capacitance must be computed using only information found in a given impedance spectra as can be done using Equation 5. This yields a mechanism of selecting all three components without using periodic time domain data. Once all values were selected, using only Fourier domain data, the error comparisons can again be made against the original computational model data. The diastolic mean flow was reconstructed to within 2% (average of all outlet cases) under rest conditions and within 5.1% (average of all outlet cases) under exercise conditions. In terms of Amplitude

Error, over all cases under rest conditions the amplitude range for blood flow is reproduced to within 8.4% and the amplitude range for blood pressure is reproduced to within 7.03%. After removing the aforementioned two outliers, these percentages decrease to within 5.4% for both blood flow and blood pressure reconstruction. This value (for pressure and flow) approximately doubles when comparing under exercise conditions. It can be noted that the reconstructions were most accurate in the larger visceral blood flow outlets while the smaller lower extremity outlets proved less accurate. The diastolic mean pressure was reconstructed to within 2% under rest conditions and within 8.2% (decreasing to 5.1% when outliers are removed) under exercise conditions.

Table 1: Example of Selected Values. The values of the resistances for all three methods, *C* optimized for flow and pressure (intermediate step), and *C* as predicted by the Fourier Method are shown in table. Computed iliac artery (exercise) data was used for this example of value selections.

Iliac Artery	***R_1*** ***(dyne•s•cm^{-5})***	***R_2*** ***(dyne•s•cm^{-5})***	***C* - Flow** ***(cm^5•dyne^{-1}•s^{-1})***	***C* - Pressure** ***(cm^5•dyne^{-1}•s^{-1})***	**Predicted *C* *(cm^5•dyne^{-1}•s^{-1})***
Method 1	3.91E+02	4.65E+03	4.46E-06	4.57E-05	
Method 2	1.11E+03	3.94E+03	9.67E-05	9.85E-05	
Method 3	1.13E+03	3.91E+03	1.04E-04	1.02E-04	5.88E-04

3.2 Two-Element Lumped Parameter Model

In the case of the simpler RC Windkessel model, the same features in the impedance phase cannot be duplicated when selecting a capacitance value. Matching the initial downslope (such as in Figure 9) proved to be important in some cases where matching the 2/3 of the phase initial upslope (as in Figure 10) proved to be more important in others. When dynamically altering *C*, with these 18 impedance spectra, there was not a common theme that yielded the best results in both blood flow and blood pressure cases. An example of this can be seen in Figure 9 where a good reconstruction of blood pressure can be seen but where blood flow is very inaccurate.

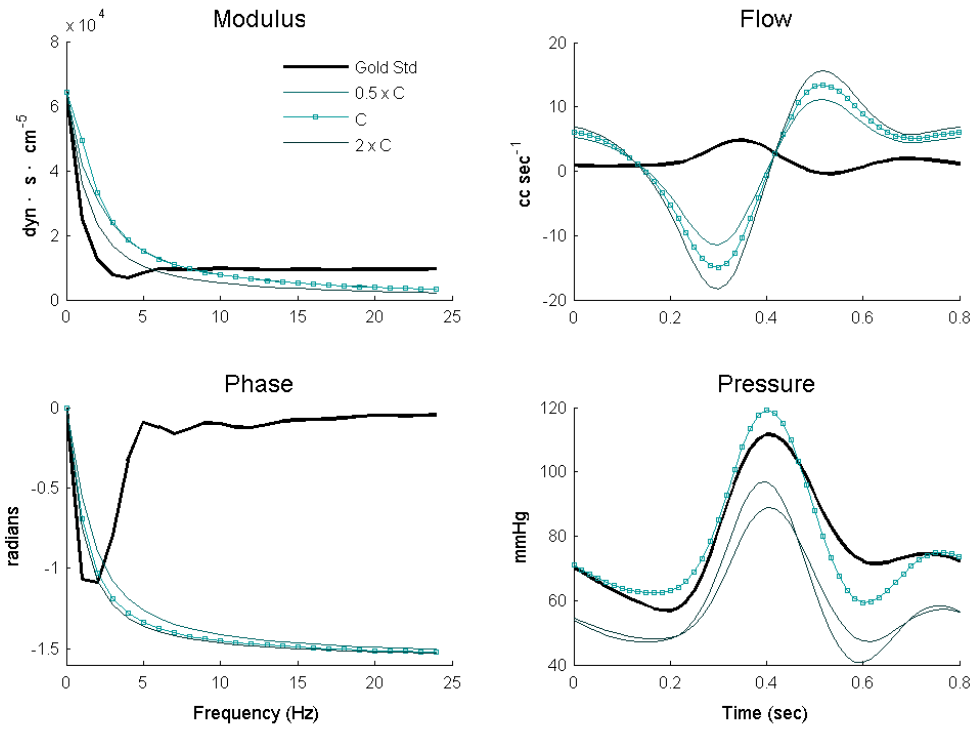

Figure 9: Dynamically Altering C in the Two-element Lumped Parameter Model – *Matching the initial downslope of the impedance phase by dynamically altering the capacitance yields a good blood pressure reconstruction for this example but the same method does not yield a reasonable blood flow reconstruction (profunda under rest conditions, Best Fit C estimated at 2.51 x10^-6 cm^5/(dyne*s)).*

Even given the most accurate capacitance value in each case there were only two cases where the RC circuit outperformed the three-element lumped parameter model in terms of both recreating the diastolic mean and the amplitude range. The RC model was generally able to reconstruct the diastolic mean but was less reliable in reconstructing an accurate amplitude range. It can be concluded that for this parameter estimation strategy using the three-element model will be the preferred method. Figure 10 illustrates a comparison of the two- and three- element cases against the original computational model data.

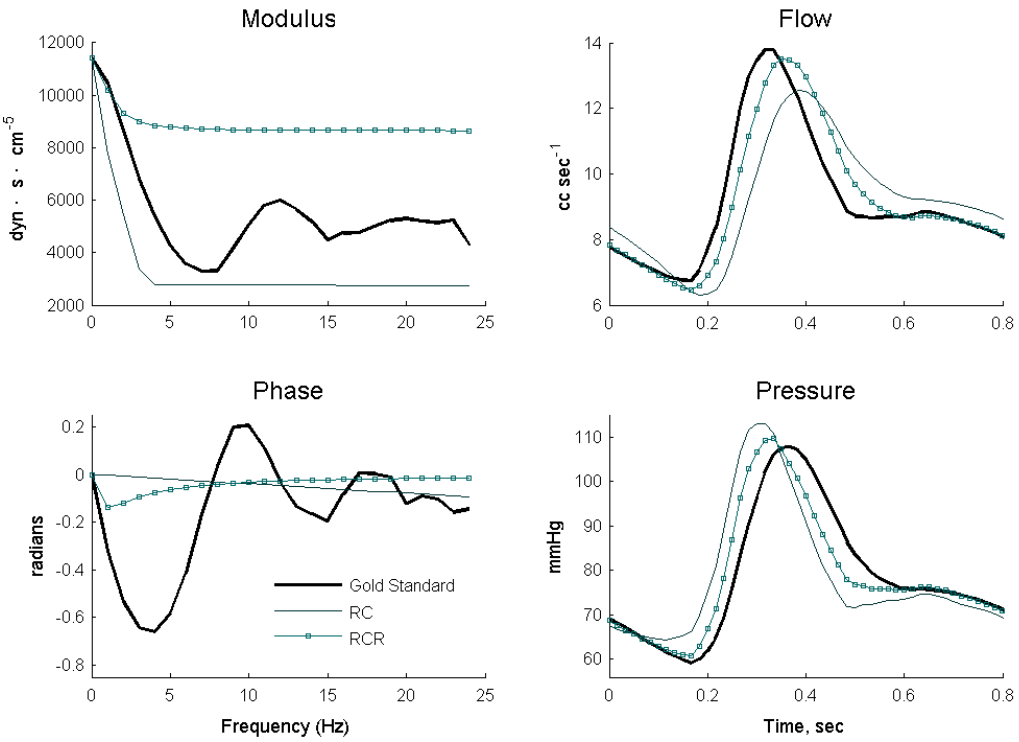

Figure 10: RCR vs. RC *– A comparison of the two-and three- element models when C is dynamically selected for the RC model vs. the computed C for the RCR model (Renal artery under rest conditions).*

3.3 Comparison of Time Domain and Fourier Domain Method

3.3.1 Comparison of Flow and Pressure Waveforms

The reconstructed flow waveforms produced by the "Fourier Method" presented above and the "Time domain method" validated by Shim et al can be compared to add one further gage of accuracy. Four examples of blood flow and pressure reconstructions using both methods and the original computational model flow and pressure waveforms are shown in Figure 11 illustrate this comparison.

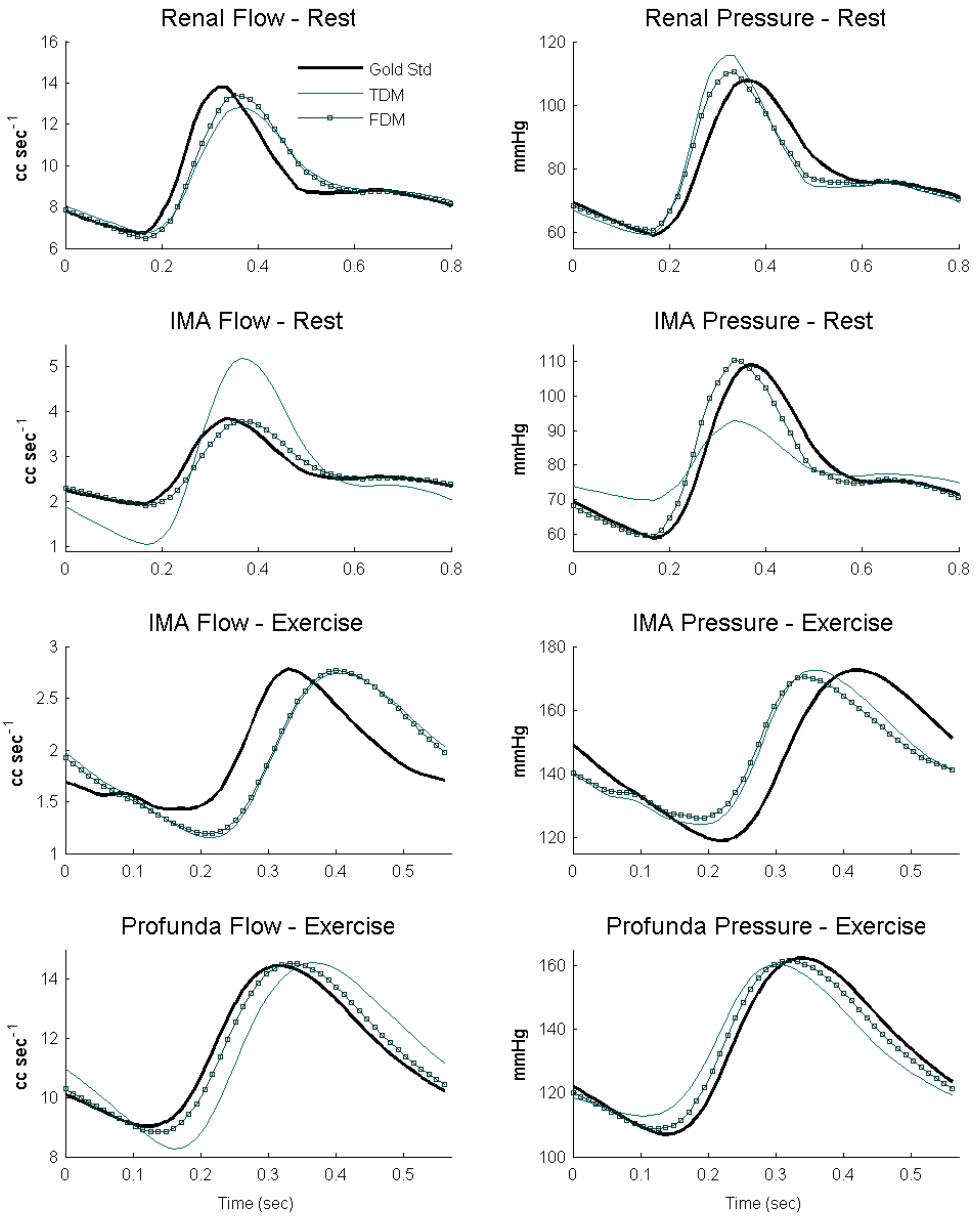

Figure 11: Time Domain Method vs. Fourier Domain Method – *Four examples of the comparison between the original computational model flow and pressure data with the blood flow and pressure waveforms reconstructed by the 'time domain method' and the 'Fourier domain method'.*

The comparisons indicate that the two methods perform comparably. In all but two cases the Fourier Domain method performed as well or better than the Time Domain method in terms of reproducing the original diastolic mean flow and pressure. In terms of recreating the amplitude error, both methods recreated the amplitude range similarly with each proving more accurate in several individual cases. For the two previously mentioned outliers, both methods continued to perform similarly with neither being better for these particular cases than the other.

CHAPTER IV

DISCUSSION AND CONCLUSIONS

4.1 Conclusions

In large computational models of vascular networks, geometric models can struggle with very large numbers of outlets. Using a lumped parameter boundary condition to represent conditions at specific outlets can alleviate some of the strain placed on such models. Lumped parameter boundary conditions have repeatedly been examined, and can accurately describe the periodic pressure-flow relations (or impedance) at the inlet of a particular arterial system.

Traditionally, electrical analogs are fit to experimental data. Periodic blood pressure and flow data is used in conjunction with Fourier domain manipulations to extract lumped parameter components. Shim et al. proposed a method of component selection which requires only calculations performed in the time domain [4]. However, the specific problems we address are the cases where no time domain data is available for arterial outlets. If such Windkessel parameters can be accurately selected using only Fourier domain data, an RCR or RC model can be an even more robust tool for representing boundary conditions at specific downstream outlets.

A selection method for RCR and RC components that is solely independent of periodic time domain data is defined using characteristics of the shape of impedance moduli and phase. Identifying Method 3, where the proximal resistor (R_1) is set to the average of the modulus terms up to the term in which the phase angle of the impedance spectra changes slope, as “best” illustrates features present in the impedance spectra that are useful for predicting resistance values, namely the range of harmonics that should be averaged. A previously discussed limitation of parameters estimated using the three-element Windkessel is that the characteristic impedance is typically underestimated and this strategy generally produces a larger estimate for this value. This slightly larger estimate appears to correspond with a smaller time delay in the blood flow and pressure waveform reconstructions. The focus of this project was to predict accurate time-domain data rather than identically matching the Fourier domain spectra. So in this work Method 3 was used to predict the characteristic impedance, though the strategy of selecting capacitance shouldn’t vary if R_1 was selected using the more traditional Method 2.

The method of choosing a capacitance value also identified key features in the impedance phase spectra, specifically the recovery time of the impedance phase after its initial minima. Initially matching the downward slope of the gold standard (computational model) data and then having a quick recovery time (where the RCR phase spectra intersected the original phase spectra at about 2/3 up the initial upslope of the phase) effected both the time lag and the amplitude reconstructed in the flow and pressure waveforms. This relationship is

illustrated in Figure 6. This Fourier selection method is consistent with the point that compliance is a low-frequency property [13, 16] and utilizes the lower frequency characteristics of the impedance phase when estimating a capacitance value.

Through the initial dynamic selection of capacitance, it can be seen that a "good" boundary condition representation is possible using an electrical analog for peripheral blood flow outlets and the ambiguity that is historically present regarding the selection of the characteristic impedance value in an RCR model can be alleviated. For this investigation, when all lumped parameter model components are selected solely from the impedance spectra the three-element model performs better than the two-element model. The results coincided with the conclusions of Wang et al and Westerhof et al [2, 20]. They document a difference between the two- and three-element Windkessel models as being that the two perform similarly during diastole (when characteristic impedance has no effect) but suffer differences during systole [2, 21].

When comparing the three-element Windkessel model to a previously published model, the results indicate that the presented methods perform comparably. The trend appears to be that selecting the parameters using the Fourier method yields better reconstructions than previous methods in the smaller (diameter) arteries which are less compliant (here the internal iliac, the profunda, etc.). Overall, however, the method is slightly more accurate in estimating the amplitude ranges (both of blood flow and pressure) when under rest conditions, as compared to exercise conditions regarding wave amplitude

error. The smoother shape of exercise condition waveforms are easier to reconstruct. This may indicate that flow rate impacts the accuracy of this modeling strategy. When arteries are under exercise conditions they expand to accommodate a higher flow rate causing a decrease in compliance. Overall, more compliant arteries yield better results (agreeing with previous studies discussed in the introduction and background as a characteristic of lumped parameter models). When attempting to adjust the parameter estimation strategy, estimating *C* based on slightly different criteria, no conclusive pattern yielded more accurate results across all less compliant vessels. This increase in error associated with increased compliance may be an inherent limitation of the type of model.

4.2 Limitations

Previously documented limitations to general lumped parameter models are also exhibited here. An example being that in the case of two-element Windkessel models, the effects of wave travel, wave reflections, etc cannot be represented. Though three-element Windkessel models are increasingly used to model the smaller peripheral arterial bed, generally they are more accurate for larger more compliant vessels [2].

Another noted limitation is the time shift that occurs between the reconstructed and original waveforms. The time lag that is inherently present between pressure and flow in systemic circulation could be the source of this

discrepancy. In the scope of this study, when given cyclic “gold standard data” and an impedance spectra, using a three-element lumped parameter model to estimate either cyclic pressure or flow yields results with a good reconstruction of waveform shape but with a consistent time lag. This also is consistent with previous work in that the phase effect present with these model types does not affect the reconstruction of wave shapes, only their time delay [2]. If this selection strategy is implemented for boundary conditions at peripheral outlets in a large hemodynamic model, whether or not these individual lags propagate backward up the model could be a source of concern.

4.3 Future Work

Three methods of selecting the resistance values based on physical characteristics of the impedance spectra are compared in this study. If other characteristics are identified as being present throughout typical impedance spectra other selection methods could be investigated, perhaps further increasing accuracy. Implementing this modeling strategy into larger more complex hemodynamic models where experimental blood flow (or pressure) data is unavailable would also be a beneficial possibility.

APPENDIX I

MATHMATICA PROGRAM

Three Methods of selecting R1, dynamically selecting C

```
(* Setting up dynamic estimation of Q, P, Modulus and Phase*)

w[k_] := 2 i k
ZRCR[R_, Rd_, C_, k_] := (R + Rd + i w[k] R Rd C)/(1 + iw[k] Rd C)
timestepsPer = 50;

loadPandQfromExperimentalData[model_, segment_] := {
 pathname = basePath <> model <> "/" <> segment <> "_Q.txt";
 tq = Import[pathname, "Table"];
 pathname = basePath <> model <> "/" <> segment <> "_P.txt";
 tp = Import[pathname, "Table"];
 t = Table[tq[[i, 1]], {i, Length[tq] - timestepsPer, Length[tq] - 1}];
 q = Table[tq[[i, 2]], {i, Length[tq] - timestepsPer, Length[tq] - 1}];
 p = Table[
  tp[[i, 2]]*1333.3332, {i, Length[tp] - timestepsPer, Length[tp] - 1}];
 Pw = Fourier[p, FourierParameters -> {1, -1}];
 Qw = Fourier[q, FourierParameters -> {1, -1}];
 Zw = Pw/Qw;
 n = Length[Pw];

 avgqData = Mean[q];
 avgpData = Mean[p];
 qAmplitudeData = Max[q] - Min[q];
 pAmplitudeData = Max[p] - Min[p];
 plotExpData;
 }

plotExpData := {
 plotQdata =
  ListLinePlot[Table[{t[[i]], q[[i]]}, {i, 1, Length[t]}],
   PlotStyle -> {Black, Thickness[.005]}, PlotRange -> All,
   AxesLabel -> {"s", "cc/s"}, PlotLabel -> "Flow"],
 plotPdata =
  ListLinePlot[Table[{t[[i]], p[[i]]}, {i, 1, Length[t]}],
```

```
   PlotStyle -> {Black, Thickness[.005]}, PlotRange -> All,
   AxesLabel -> {"s", "dynes s /cm^2"}, PlotLabel -> "Pressure"],
  plotAbsData =
   ListLinePlot[Table[Abs[Zw[[i]]], {i, 1, n/2}],
    PlotStyle -> {Black, Thickness[.005]}, PlotRange -> All,
    PlotLabel -> "Modulus"],
  plotArgData =
   ListLinePlot[Table[Arg[Zw[[i]]], {i, 1, n/2}],
    PlotStyle -> {Black, Thickness[.005]}, PlotRange -> All,
    PlotLabel -> "Phase"]
  }


qForRCR[R1_, R2_, C1_] := {
   ztest = Table[ZRCR[R1, R2, C1, k], {k, 0, n - 1}];
   Qtest = Pw/ztest;
   qtest = Re[InverseFourier[Qtest, FourierParameters -> {1, -1}]]
   }[[1]]
pForRCR[R1_, R2_, C1_] := {
   ztest = Table[ZRCR[R1, R2, C1, k], {k, 0, n - 1}];
   Ptest = Qw*ztest;
   ptest = Re[InverseFourier[Ptest, FourierParameters -> {1, -1}]]
   }[[1]]

plotQForRCR[R1_, R2_, C1_, plotColor_] := {
  (* compare  orig flow data using impedance *)
  qForRCR[R1, R2, C1];
  plotqtest =
   ListLinePlot[Table[{t[[i]], qtest[[i]]}, {i, 1, Length[t]}],
    PlotStyle -> {  plotColor, Thickness[.005]}, PlotRange -> All,
    AxesLabel -> {"s", "cc/s"}, PlotLabel -> "Test Flow"];
  Show[plotQdata, plotqtest, PlotRange -> All],


  plotAbsTest =
   ListLinePlot[Table[Abs[ztest[[i]]], {i, 1, n/2}],
    PlotStyle -> {  plotColor, Thickness[.005]}];
  Show[plotAbsData, plotAbsTest],
  plotArgTest =
   ListLinePlot[Table[Arg[ztest[[i]]], {i, 1, n/2}],
    PlotStyle -> {  plotColor, Thickness[.005]}];
  Show[plotArgData, plotArgTest],
```

```
 qErrorMean = avgqData - Mean[qtest];
 qAmplitudeTest = Max[qtest] - Min[qtest];
 qErrorAmplitude = (qAmplitudeData - qAmplitudeTest)/qAmplitudeData * 100,
 qErrorRMS = RootMeanSquare[q - qtest],
 dc
 }

plotPForRCR[R1_, R2_, C1_, plotColor_] := {
 (* compare  orig flow data using impedance *)
 pForRCR[R1, R2, C1];
 plotptest =
  ListLinePlot[Table[{t[[i]], ptest[[i]]}, {i, 1, Length[t]}],
   PlotStyle -> {  plotColor, Thickness[.005]}, PlotRange -> All,
   AxesLabel -> {"s", "dyne s/cm^2"}, PlotLabel -> "Pressure"];
 Show[plotPdata, plotptest, PlotRange -> All],

 plotAbsTest =
  ListLinePlot[Table[Abs[ztest[[i]]], {i, 1, n/2}],
   PlotStyle -> {  plotColor, Thickness[.005]}];
 Show[plotAbsData, plotAbsTest],
 plotArgTest =
  ListLinePlot[Table[Arg[ztest[[i]]], {i, 1, n/2}],
   PlotStyle -> {  plotColor, Thickness[.005]}];
 Show[plotArgData, plotArgTest],
 pErrorMean = avgpData - Mean[ptest];
 pAmplitudeTest = Max[ptest] - Min[ptest];
 pErrorAmplitude = (pAmplitudeData - pAmplitudeTest)/pAmplitudeData *100,
 pErrorRMS = RootMeanSquare[p - ptest],
 dc
 }


basePath = "/Users/leperkin/Model/";
eData = loadPandQfromExperimentalData["Crest", "LSceliac.scaled.1.30"];
dummyData = loadDummyPandQ["Crest", "LSaorta.scaled.0.0"];

est1R1 = Min[Abs[Zw]]
hoterms =
 Table[Abs[Zw[[i]]], {i, 2, 25}];(* 2 -> # of minimum Modulus *)
est2R1 =
 Mean[hoterms]
hoterms =
```

```
 Table[Abs[Zw[[i]]], {i, 0, 5}]; (* 5 -> # of minimum phase angle *)
est3R1 =
 Mean[hoterms]

MyDynamic = {(*Slider[Dynamic [dr] ,{5000,9000}]*)  dr = est3R1,
 Dynamic[r2 = Re[Zw[[1]]] - dr]
  Slider[Dynamic[dc] , {3.67 *10 ^ -6, 1.44*10 ^-4}],
 Dynamic[plotQForRCR[dr, r2, dc, Green]],
 Dynamic[plotPForRCR[dr, r2, dc, Red]]}
```

```
{5275.03, 4429.08
```

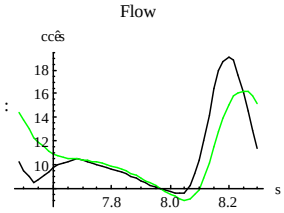

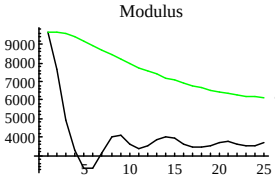

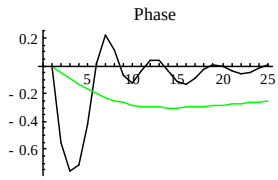


```
, 18.9758, 2.24082, 3.67¥10^-6>
```

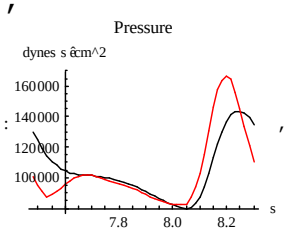

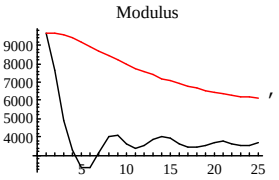

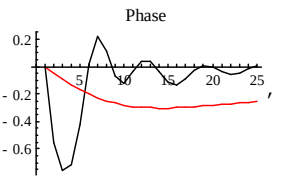


```
, - 31.3516, 15539., 3.67¥10^-6>
}
```

```
(*C PROGRESSION  - RCR*)

GoodQ = qForRCR[est3R1, Zw[[1]] - est3R1, 8.05* 10^-5];
GoodP = pForRCR[est3R1, Zw[[1]] - est3R1, 8.05* 10^-5];
GoodMod = Table[Abs[ztest[[i]]], {i, 1, n/2}];
GoodPhase = Table[Arg[ztest[[i]]], {i, 1, n/2}];
SmallCQ = qForRCR[est3R1, Zw[[1]] - est3R1, 1* 10^-5];
SmallCP = pForRCR[est3R1, Zw[[1]] - est3R1, 1* 10^-5];
SmallCMod = Table[Abs[ztest[[i]]], {i, 1, n/2}];
SmallCPhase = Table[Arg[ztest[[i]]], {i, 1, n/2}];
BigCQ = qForRCR[est3R1, Zw[[1]] - est3R1, 1* 10^-4];
BigCP = pForRCR[est3R1, Zw[[1]] - est3R1, 1* 10^-4];
BigCMod = Table[Abs[ztest[[i]]], {i, 1, n/2}];
BigCPhase = Table[Arg[ztest[[i]]], {i, 1, n/2}];
OrigMod = Table[Abs[Zw[[i]]], {i, 1, n/2}];
```

```
OrigPhase = Table[Arg[Zw[[i]]], {i, 1, n/2}];

Export["Cprogression.xls", {OrigMod, OrigPhase, , t, q, SmallCQ, GoodQ,
  BigCQ, , p, SmallCP, GoodP, BigCP, , SmallCMod, GoodMod, BigCMod, ,
  SmallCPhase, GoodPhase, BigCPhase}, "XLS"];

(*SHIM COMPARISON RCR *)
ShimR = 4.62*10^3;
ShimC = 4.76* 10^-7;
FourierC = 1.12* 10^-4;
TimeMethodQ = qForRCR[ShimR, Zw[[1]] - ShimR, ShimC];
FourierMethodQ = qForRCR[est3R1, Zw[[1]] - est3R1, FourierC];
TimeMethodP = pForRCR[ShimR, Zw[[1]] - ShimR, ShimC];
FourierMethodP = pForRCR[est3R1, Zw[[1]] - est3R1, FourierC];
Export["TimevsIntegral.xls", {t, q, TimeMethodQ, FourierMethodQ, , p,
  TimeMethodP, FourierMethodP}, "XLS"];
```

APPENDIX II

MATLAB PROGRAMS

1. Implementing Time Domain Method

```
% Integral Method for estimating RCR - (Shim Paper)

%Importing Data
Flow = load ('~/Model/Crest/LSr.renal.scaled.1.30_Q.txt');
qcycle = Flow(:,2);
Pressure = load ('~/Model/Crest/LSr.renal.scaled.1.30_P.txt');
pcycle = Pressure(:,2);

% Only need one cycle of the flow and pressure (50 datapoints)
qcycle = qcycle(length(qcycle)-59:length(qcycle)-10);
pcycle = pcycle(length(pcycle)-59:length(pcycle)-10);
time = Flow(1:50,1);

%Plot of One cycle - Pressure and Flow
 subplot (1,2,1)
 plot (time, qcycle)
 xlabel('time - sec')
 ylabel ('Flow')
 subplot (1,2,2)
 plot (time, pcycle)
 xlabel ('time - sec')
 ylabel ('Pressure')

% INTEGRAL METHOD

%getting the pulsatile pressure amplitude  - Pcycle minus end
%dyastolic pressure

%Need to choose 6-8 points to make a comparison - (from the
ejection point)
%-not the whole cycle

%need to multiply the pressure by 1333.33 to convert to dynes
ratio = 0;
i=1;
for tk = 15:2:15;
    Ped = (min(pcycle))*1333.33;
    PPA(i) = pcycle(tk)*1333.33 - Ped;
    Qpoints(i) = qcycle(tk);
    ratio = ratio+PPA(i)/Qpoints(i);
    i = i+1;
end
```

```
Zch = 1/(i-1)*ratio

%calculating  resistance  (R2)
%again need to multiply the pressure by 1333.33 - converting to
dynes
Pmean = mean(pcycle)*1333.33;
Qmean = mean(qcycle);

R = (Pmean./Qmean) - Zch

%To calculate compliance:
%need to best-fit the curves and get a polynomial that can be
integrated
%paper only considered the flow and pressure during early
ejection, only look at points 5-15 (will change) like before
figure
subplot (1,2,1)
plot (time(15:25), qcycle(15:25))
xlabel('time - sec')
ylabel ('Flow')
subplot (1,2,2)
%%Again scale the pressure
plot (time(15:25), pcycle(15:25)*1333.33)
xlabel ('time - sec')
ylabel ('Pressure')

%From above, use best-fit equation for pressure and
% for flow - get from figure tools
syms p q;

%%Renal
Pfit = 1.404e7*p^3+-7.0276e6*p^2+8.5519e5*p+1.1329e5;
Qfit = 96.254*q^2-59.309*q+17.081;

%integrate the bestfit polynomials for pressure (pfit) and flow
%(qfit)
t2 = 0.15;
t1 = 0.25; %Check this - these 2 points mark early ejection
(beginning and end times)
Pint = int(Pfit);
Psub = subs(Pint,p,t2) - subs(Pint,p,t1);
Qint = int(Qfit);
Qsub = subs(Qint,q,t2) - subs(Qint,q,t1);

%%Calculate C
Cu = (Psub-((R+Zch)*Qsub));
Cl = R*(pcycle(15) - pcycle(25)) - R*Zch*(qcycle(15) -
qcycle(25));
C = Cu/Cl
```

2. Calculate C using Fourier Method

```
%% Calculate C value from Impedance Mod and Phase

R1=5936.76;
R2=6518.28;
w=15;
Angle = -.175178569;
ZMag = 4907.674601;
syms C %R1 R2 w

Z = ZMag* exp(i*Angle);
%Z=(R1 + R2 + i*w*R1*R2*C)/(1+i*w*R2*C)

Answer = solve(((R1 + R2 + i*w*R1*R2*C)/(1+i*w*R2*C))^2 -
Z^2,'C');
Answer = simplify(Answer)

C1 = (Z-R1 - R2)/(w*R1*R2*i-Z*i*w*R1)
C2 = abs(C1)
```

****** Matlab Also Used to Create Figures 2-11

References

[1] Silverthorn, D.U., 2006, "Human Physiology An Integrated Approach," Pearson Education Inc. as Benjamin Cummingso, San Francisco, CA, pp. 859.

[2] Westerhof, N., Lankhaar, J. W., and Westerhof, B. E., 2009, "The Arterial Windkessel," Medical & Biological Engineering & Computing, **47**(2) pp. 131-141.

[3] Stergiopulos, N., Meister, J. J., and Westerhof, N., 1995, "Evaluation of Methods for Estimation of Total Arterial Compliance," The American Journal of Physiology, **268**(4 Pt 2) pp. H1540-8.

[4] Shim, Y., Pasipoularides, A., Straley, C. A., 1994, "Arterial Windkessel Parameter Estimation: A New Time-Domain Method," Annals of Biomedical Engineering, **22**(1) pp. 66-77.

[5] Avanzolini, G., Barbini, P., Cappello, A., 1989, "Electrical Analogs for Monitoring Vascular Properties in Artificial Heart Studies," IEEE Transactions on Bio-Medical Engineering, **36**(4) pp. 462-470.

[6] Steele, B. N., Olufsen, M. S., and Taylor, C. A., 2007, "Fractal Network Model for Simulating Abdominal and Lower Extremity Blood Flow during Resting and Exercise Conditions," Computer Methods in Biomechanics and Biomedical Engineering, **10**(1) pp. 39-51.

[7] O'Rourke, M. F., 1982, "Vascular Impedance in Studies of Arterial and Cardiac Function," Physiological Reviews, **62**(2) pp. 570-623.

[8] Adamson, S. L., 1999, "Arterial Pressure, Vascular Input Impedance, and Resistance as Determinants of Pulsatile Blood Flow in the Umbilical Artery," European Journal of Obstetrics, Gynecology, and Reproductive Biology, **84**(2) pp. 119-125.

[9] Avolio, A., 2009, "Input Impedance of Distributed Arterial Structures as used in Investigations of Underlying Concepts in Arterial Haemodynamics," Medical & Biological Engineering & Computing, **47**(2) pp. 143-151.

[10] Mills, C. J., Gabe, I. T., Gault, J. H., 1970, "Pressure-Flow Relationships and Vascular Impedance in Man," Cardiovascular Research, **4**(4) pp. 405-417.

[11] Frank, O., 1889, "Die Grundform Des Arteriellen Pulses," Z Biol, **37**.

[12] Stergiopulos, N., Meister, J. J., and Westerhof, N., 1994, "Simple and Accurate Way for Estimating Total and Segmental Arterial Compliance: The Pulse Pressure Method," Annals of Biomedical Engineering, **22**(4) pp. 392-397.

[13] Segers, P., Brimioulle, S., Stergiopulos, N., 1999, "Pulmonary Arterial Compliance in Dogs and Pigs: The Three-Element Windkessel Model Revisited," The American Journal of Physiology, **277**(2 Pt 2) pp. H725-31.

[14] Olufsen, M. S., 1999, "Structured Tree Outflow Condition for Blood Flow in Larger Systemic Arteries," The American Journal of Physiology, **276**(1 Pt 2) pp. H257-68.

[15] Cappello, A., Gnudi, G., and Lamberti, C., 1995, "Identification of the Three-Element Windkessel Model Incorporating a Pressure-Dependent Compliance," Annals of Biomedical Engineering, **23**(2) pp. 164-177.

[16] Quick, C. M., Berger, D. S., and Noordergraaf, A., 1998, "Apparent Arterial Compliance," The American Journal of Physiology, **274**(4 Pt 2) pp. H1393-403.

[17] Dujardin, J. P., and Stone, D. N., 1981, "Characteristic Impedance of the Proximal Aorta Determined in the Time and Frequency Domain: A Comparison," Medical & Biological Engineering & Computing, **19**(5) pp. 565-568.

[18] Lucas, C. L., Wilcox, B. R., Ha, B., 1988, "Comparison of Time Domain Algorithms for Estimating Aortic Characteristic Impedance in Humans," IEEE Transactions on Bio-Medical Engineering, **35**(1) pp. 62-68.

[19] Wan, J., Steele, B., Spicer, S. A., 2002, "A One-Dimensional Finite Element Method for Simulation-Based Medical Planning for Cardiovascular Disease," Computer Methods in Biomechanics and Biomedical Engineering, **5**(3) pp. 195-206.

[20] Womersley, J. R., 1957, "Oscillatory Flow in Arteries: The Constrained Elastic Tube as a Model of Arterial Flow and Pulse Transmission," Physics in Medicine and Biology, **2**(2) pp. 178-187.

[21] Wang, J. J., O'Brien, A. B., and Shrive, N. G., 2003, "Time-Domain Representation of Ventricular-Arterial Coupling as a Windkessel and Wave System," American Journal of Physiology Heart Circulation Physiology, **284**(4) pp. H1358-68.